RESEARCH ARTICLES

PRIMATE EVOLUTION

Oligocene primates from China reveal divergence between African and Asian primate evolution

Xijun Ni,[1,2]* Qiang Li,[1,2] Lüzhou Li,[1] K. Christopher Beard[3,4]

Profound environmental and faunal changes are associated with climatic deterioration during the Eocene-Oligocene transition (EOT) roughly 34 million years ago. Reconstructing how Asian primates responded to the EOT has been hindered by a sparse record of Oligocene primates on that continent. Here, we report the discovery of a diverse primate fauna from the early Oligocene of southern China. In marked contrast to Afro-Arabian Oligocene primate faunas, this Asian fauna is dominated by strepsirhines. There appears to be a strong break between Paleogene and Neogene Asian anthropoid assemblages. Asian and Afro-Arabian primate faunas responded differently to EOT climatic deterioration, indicating that the EOT functioned as a critical evolutionary filter constraining the subsequent course of primate evolution across the Old World.

Primates are among the most thermophilic and hence environmentally sensitive of all mammals. As a result, both the geographic distribution and macroevolutionary patterns shown by fossil primates are strongly mediated by shifting climatic conditions during the Cenozoic. Dramatic range expansions, such as the dispersal of the earliest primates from their Asian birthplace into North America and Europe during the Paleocene-Eocene Thermal Maximum, coincided with intervals of extreme global warmth (*1*, *2*). In contrast, episodes of cooler, drier climatic conditions such as that characterizing the Eocene-Oligocene transition (EOT) resulted in continental-scale extinction of primates on landmasses that lacked direct geographic access to low-latitude refugia (*3*). Primates were extirpated at or near the EOT in North America and Europe, but Afro-Arabian primate faunas dominated by anthropoids continued to radiate during the Oligocene and Neogene (*4*–*7*). In northern China and Mongolia, mammalian faunal turnover across the EOT was pervasive enough to be compared with the European Grande Coupure, and this abrupt change in Asian mammal faunas has been designated the Mongolian Remodeling (*8*, *9*). However, assessing the impact of EOT climatic deterioration on early Asian primates has been hindered by geographic and temporal biases in the Asian fossil record. Eocene primates have been sporadically reported from northern China and Mongolia (*10*–*12*), but Eocene primates are more diverse and abundant in southern Asia, where the Oligocene record is generally absent (*13*, *14*). With the sole exception of the late early Oligocene Paali Nala locality in the Bugti Hills of Pakistan (*15*–*17*), Oligocene primates are unknown in Asia. This very limited record of Asian Oligocene primates has made it difficult to assess the impact of EOT environmental changes on Asian primate evolution. Here, we describe a diverse assemblage of fossil primates from the early Oligocene of Yunnan Province in southern China that helps to fill this gap in the record of Asian primate evolution.

We collected the primate fossils reported here via careful excavation and screen-washing at the Lijiawa fossil site in Yunnan, which has yielded more than 10 mammal taxa that indicate an early Oligocene age (supplementary materials) (*18*).

Primates Linnaeus, 1758; Strepsirhini Geoffroy, 1812; Adapiformes Hoffstetter, 1977; Sivaladapidae Thomas and Verma, 1979; *Yunnanadapis* gen. nov. **Type species**: *Yunnanadapis folivorus* sp. nov. **Included species**: The type species and *Yunnanadapis imperator* sp. nov. **Diagnosis**: Differs from *Paukkaungia*, *Hoanghonius*, and *Rencunius* in having more nearly molariform P_4 and P^4 (P^4 remains unknown in *Paukkaungia*). Lower molars further differ from those of *Paukkaungia*, *Hoanghonius*, and *Rencunius* in having less cuspidate paraconids and more angular hypoconids that are relatively mesial in position, so that the cristid obliqua is shorter than the postcristid. Upper molars further differ from those of *Hoanghonius* and (especially) *Rencunius* in lacking distinct conules. Lower molars differ from those of *Wailekia* and *Kyitchaungia* in having lingually open trigonids with protoconid and metaconid more closely approximated and talonids bearing more trenchant cristids. Upper molars differ from those of *Guangxilemur* in having more prominent parastyles and pre- and postprotocristae joining the bases of the paracone and metacone, respectively, rather than merging with the pre- and postcingula. Upper molars with weaker buccal cingulum and incomplete mesostyle, in contrast to *Guangxilemur tongi*. Lower molars differ from those of *Guangxilemur singsilai* in having lingually open trigonids and deeper, more extensive valley separating entoconid and hypoconulid. Differs from Miocene sivaladapids in lacking fully molariform P_4 and P^4 and having upper molars with distinct pericone and hypocone cusps and pre- and postprotocristae joining bases of paracone and metacone. **Etymology**: Generic name recognizes the geographic provenance of this taxon and its adapiform affinities.

Yunnanadapis folivorus sp. nov. **Holotype**: IVPP V22702, left dentary fragment preserving the crowns of C_1-M_3 (Fig. 1A and supplementary materials). **Horizon and locality**: Early Oligocene Lijiawa fossil site, upper part of Caijiachong Formation, Yuezhou Basin, Yunnan Province, China. **Diagnosis**: Smaller than *Yunnanadapis imperator*. P_3 without buccal cingulid, in contrast to *Y. imperator*. P_4 differs from that of *Y. imperator* in having much weaker buccal cingulid and hypoconid and cristid obliqua more lingual in position, yielding deeper hypoflexid and narrower talonid basin. **Etymology**: Trivial name reflects the likely dietary adaptations of this species.

Yunnanadapis imperator sp. nov. **Holotype**: IVPP V22706, right P_4 (Fig. 1B and supplementary materials). **Horizon and locality**: Early Oligocene Lijiawa fossil site, upper part of Caijiachong Formation, Yuezhou Basin, Yunnan Province, China. **Diagnosis**: Larger than *Yunnanadapis folivorus*. P_3 with strong buccal cingulid, in contrast to *Y. folivorus*. P_4 differs from that of *Y. folivorus* in having much stronger buccal cingulid and hypoconid and cristid obliqua more buccal in position, yielding shallower hypoflexid and wider talonid basin. **Etymology**: Latin "imperator" (commander), in allusion to the large size of this species.

Laomaki yunnanensis gen. et sp. nov. **Holotype**: IVPP V22708, right maxilla fragment preserving $M^{1\text{-}3}$ (Fig. 1C and supplementary materials). **Horizon and locality**: Early Oligocene Lijiawa fossil site, upper part of Caijiachong Formation, Yuezhou Basin, Yunnan Province, China. **Diagnosis**: Differs from all sivaladapids aside from *Rencunius* in having strongly developed conules on upper molars. P_4 and P^4 lack substantial molarization, in contrast to *Yunnanadapis* and Miocene sivaladapids. Upper and lower molars differ from those of *Rencunius* and *Paukkaungia* in having highly crenulated enamel, taller and more pyramidal cusps/cuspids, and more trenchant crests/cristids. Upper molars are more transverse than those of *Rencunius*, and upper molar conules are pyramidal rather than bulbous. P^4 bears

[1]Key Laboratory of Vertebrate Evolution and Human Origins, Institute of Vertebrate Paleontology and Paleoanthropology (IVPP), Chinese Academy of Sciences, 142 Xi Zhi Men Wai Street, Beijing, 100044, China. [2]Chinese Academy of Sciences (CAS) Center for Excellence in Tibetan Plateau Earth Sciences, Beijing, 100101, China. [3]Biodiversity Institute, University of Kansas, 1345 Jayhawk Boulevard, Lawrence, KS 66045-7561, USA. [4]Department of Ecology and Evolutionary Biology, University of Kansas, 1345 Jayhawk Boulevard, Lawrence, KS 66045-7561, USA.
*Corresponding author. Email: nixijun@ivpp.ac.cn

a tiny hypocone, in contrast to that of *Rencunius*. **Etymology**: Generic name derives from the Mandarin "lao" (old) and the Malagasy "maky" (lemur). Trivial name reflects the geographic provenance of this species.

Ekgmowechashalidae Szalay, 1976; *Gatanthropus micros* gen. et sp. nov. **Holotype**: IVPP V22717, isolated left M_1 (Fig. 1D and supplementary materials). **Horizon and locality**: Early Oligocene Lijiawa fossil site, upper part of Caijiachong Formation, Yuezhou Basin, Yunnan Province, China. **Diagnosis**: Differs from other ekgmowechashalid primate genera (including *Bugtilemur*, *Muangthanhinius*, and *Ekgmowechashala*) in having simpler, more nearly premolariform P_4 with hypconid and cristid obliqua located near the midline of the talonid, rather than buccally as in *Bugtilemur* and *Muangthanhinius*. P_4 without neomorphic buccal cingular cuspid, in contrast to *Ekgmowechashala*. M_{1-2} lack prominent development of metastylids, in contrast to *Ekgmowechashala*. Protoconid, protocristid, and metaconid of lower molar are transversely aligned, in contrast to those of *Bugtilemur* and *Muangthanhinius*, in which these structures are obliquely oriented so that metaconid is located distolingual to protoconid. Upper molars differ from those of *Bugtilemur* in having more inflated (rather than buccolingually compressed) paracone and metacone, broader buccal cingulum, and stronger and more extensive postprotocingulum. **Etymology**: In allusion to the ekgmowechashalid affinities of this taxon, its generic name derives from the Greek "gata" (cat) and "anthropus" (man), and its trivial name derives from the Greek "micros" (small). *Ekgmowechashala* signifies "little cat man" in the Lakota language, which lacks a term for nonhuman primates.

Haplorhini Pocock, 1918; Tarsiiformes Gregory, 1915; Tarsiidae Gray, 1825; *Oligotarsius rarus* gen. et sp. nov. **Holotype**: IVPP V22727, isolated left M_1 (Fig. 1E and supplementary materials). **Horizon and locality**: Early Oligocene Lijiawa fossil site, upper part of Caijiachong Formation, Yuezhou Basin, Yunnan Province, China. **Diagnosis**: Smaller than other living and fossil tarsiers, aside from Eocene *Tarsius eocaenus* and modern *Tarsius pumilus*. Differs from extant tarsiids and Miocene *Hesperotarsius* in having well-developed conules and distobuccally oriented postmetacrista on M^1. Postprotocrista of M^1 continuous with postmetaconule crista, rather than merging with hypometacrista to form distal margin of trigon, as in extant tarsiids. M_1 differs from that of Eocene *Xanthorhysis* in being relatively shorter, broader, and higher-crowned, with entoconid located farther mesially. Lacks hypoparacrista and hypometacrista. **Etymology**: Generic name reflects the age of this taxon. Trivial name reflects the sparse documentation of Tarsiidae in the fossil record generally, as well as the meager representation of this species in the Caijiachong early Oligocene fauna.

Anthropoidea Mivart, 1864; Eosimiidae Beard *et al*., 1994; *Bahinia* Jaeger *et al*., 1999; *Bahinia banyueae* sp. nov. **Holotype**: IVPP V22730, isolated right M^1 (Fig. 1F and supplementary materials, comments regarding possible additional elements pertaining to the holotype). **Horizon**

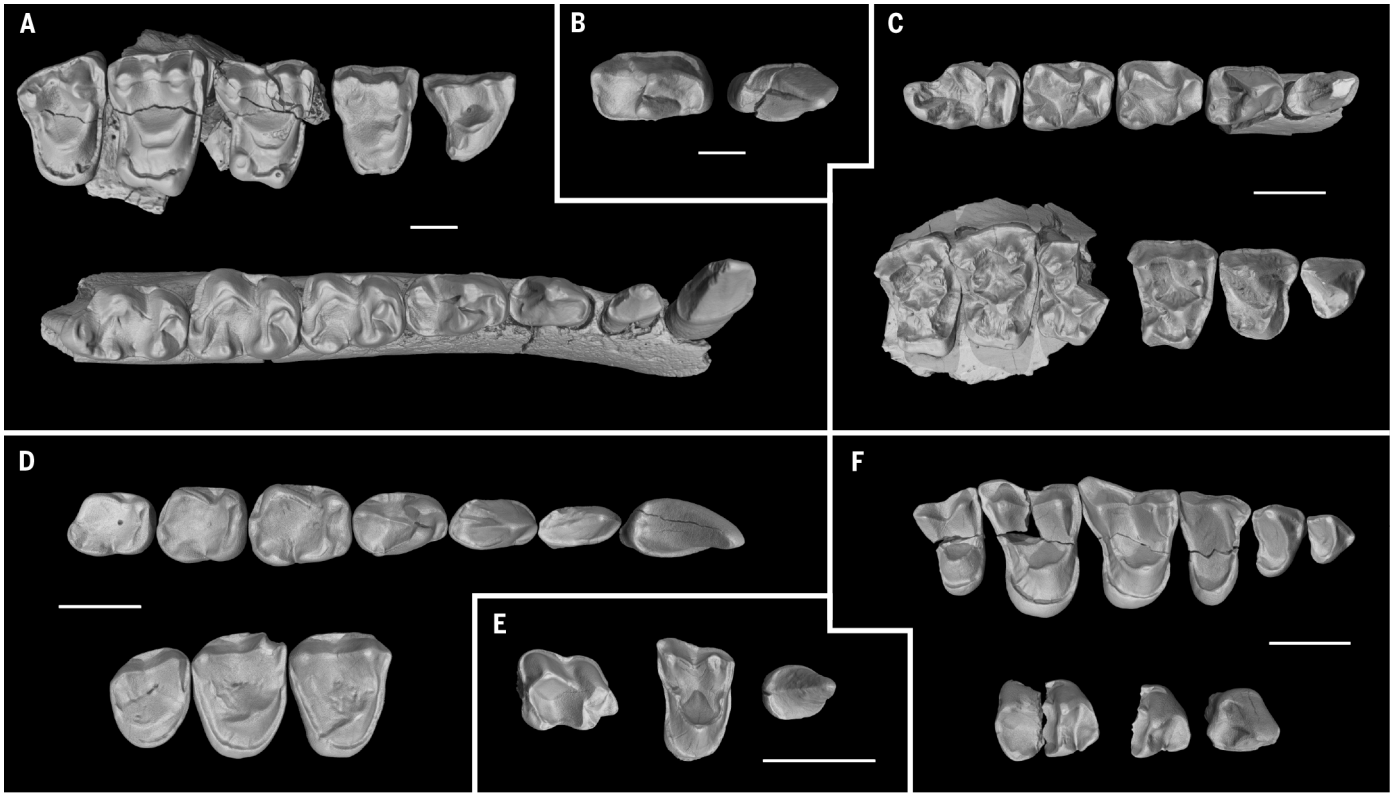

Fig. 1. Diverse primates from the early Oligocene of Yunnan Province, China. (**A**) *Yunnanadapis folivorus* gen. et sp. nov., left dentary fragment preserving C_1-M_3 (holotype, IVPP V22702), and composite upper dentition including right dP^4 (IVPP V22703), reversed left P^4 (IVPP V22704), and right maxillary fragment preserving M^{1-3} (IVPP V22705). (**B**) *Yunnanadapis imperator* gen. et sp. nov., left P_3 (IVPP V22707), and reversed right P_4 (holotype, IVPP V22706). (**C**) *Laomaki yunnanensis* gen. et sp. nov., right maxillary fragment preserving M^{1-3} (holotype, IVPP V22708); reversed left P^3, P^4, and M^1 (IVPP V22714, V22715, and V22716, respectively); reversed right dentary fragment preserving P_3, P_4, M_1, M_2, and M_3 (IVPP V22709, V22710, V22711, V22712, and V22713, respectively). (**D**) *Gatanthropus micros* gen. et sp. nov., left C_1 (IVPP V22718); reversed right P_2, P_3, P_4 (IVPP V22719, V22720, and V22721, respectively); left M_1 (holotype, IVPP V22717); left M_2 and M_3 (IVPP V22722 and V22723, respectively); right M^1, M^2, and M^3 (IVPP V22724, V22725, and V22726, respectively). (**E**) *Oligotarsius rarus* gen. et sp. nov., reversed left C^1 and M^1 (IVPP V22728 and V22729, respectively), and left M_1 (holotype, IVPP V22727). (**F**) *Bahinia banyueae* sp. nov., reversed left P^2 and P^3 (IVPP V22731 and V22732, respectively), right P^4 (IVPP V22733), right M^1 (holotype, IVPP V22730), right M^2 missing metacone lobe (IVPP V22734) juxtaposed with a right M^2 fragment preserving metacone lobe only (IVPP V22735), right M^3 (IVPP V22736), left P_3 and left trigonid of M_1 (IVPP V22737 and V22738, respectively), reversed right M_2 trigonid and talonid (IVPP V22739 and V22740, respectively). Scale bars, 2 mm.

and locality: Early Oligocene Lijiawa fossil site, upper part of Caijiachong Formation, Yuezhou Basin, Yunnan Province, China. **Diagnosis**: Upper molars with weaker buccal and lingual cingula than in *Bahinia pondaungensis*. Although $P^2 < P^3 < P^4$ as in *B. pondaungensis*, in *B. banyueae* P^2 is larger and P^3 is smaller in relation to P^4 than is the case in *B. pondaungensis*. **Etymology**: Trivial name honors the pioneering work on the Caijiachong mammal faunas of Yunnan Province made by our friend and colleague Banyue Wang.

Despite the dramatic faunal turnover during the EOT observed across Europe, North America, and northern Asia (*8*, *9*), the early Oligocene primate fauna from Yunnan reported here and the late early Oligocene primate fauna from Pakistan (*15*–*17*) show that multiple primate lineages successfully weathered the EOT climatic deterioration in tropical regions of Asia (Fig. 2). Indeed, most of the Asian primate clades that succeeded in traversing the EOT were able to persist there for tens of millions of years, showing that the EOT functioned as a critical filtering episode during the evolutionary history of Asian primates. Comparing the composition of the early Oligocene primate faunas from Yunnan and Pakistan with later Eocene Asian primate faunas known from China, Myanmar, and Thailand reveals that surviving this Eocene-Oligocene evolutionary filter entailed a high degree of taxonomic and ecological selectivity. Later Eocene primate assemblages in China, Myanmar, and Thailand tend to be dominated, both in terms of taxonomic richness and numerical abundance, by stem anthropoids belonging to the families Eosimiidae and Amphipithecidae (*13*, *14*, *19*, *20*). In stark contrast, only one of the six primates known from the early Oligocene of Yunnan is an anthropoid. Three of five primate species documented from the late early Oligocene of Pakistan are anthropoids, but even in this case, the anthropoid taxa known from Pakistan differ from their contemporary African relatives in being relatively small-bodied. Phylogenetic analysis (Fig. 3) shows that *Yunnanadapis folivorus*, *Y. imperator*, and *Laomaki yunnanensis* belong to the Sivaladapidae, a clade that persisted in southern and southeastern Asia until the late Miocene (*21*, *22*). Likewise, the affinities of *Gatanthropus micros* lie with *Muangthanhinius*, *Bugtilemur*, and the enigmatic North American genus *Ekgmowechashala*, which together comprise the strepsirhine clade Ekgmowechashalidae (*23*). Late Eocene–early Oligocene primates from Afro-Arabia show a very different pattern of taxonomic selectivity in response to the EOT. There, very few strepsirhines (none of which were large) survived the EOT, whereas anthropoids diversified both taxonomically and ecologically (Fig. 2) (*6*).

On the basis of the current record of early Oligocene primates from Yunnan, taxonomic selectivity across the EOT in southern Asia strongly

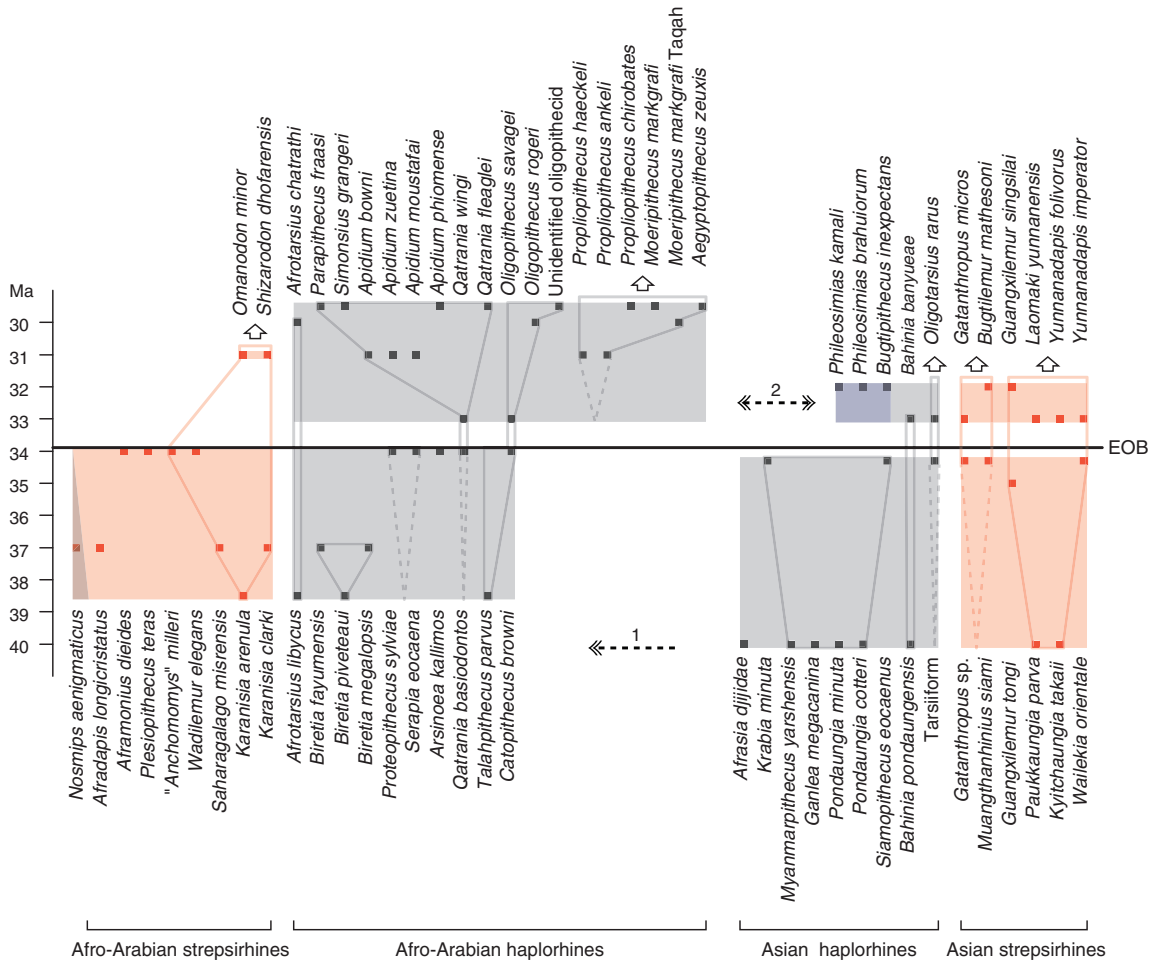

Fig. 2. Divergent taxonomic composition of fossil primates across the Eocene-Oligocene boundary (EOB) in Afro-Arabia and southern Asia. Gray area indicates haplorhines. Pale red area indicates strepsirhines. The phylogenetic affinities of *Nosmips* are uncertain (*26*). The width of the shaded areas directly reflects taxonomic diversity. Solid red and gray lines designate generally accepted monophyletic groups (Fig. 3) (*6*). Dashed lines indicate hypothetical range extensions in earlier strata. White arrows indicate that lineages persist to later intervals. Dashed line with arrowhead 1 indicates intercontinental dispersal of early anthropoids from Asia to Afro-Arabia (*6*, *27*). Dashed line with arrowhead 2 indicates a second dispersal episode of anthropoids between Afro-Arabia and Asia during the early Oligocene, as suggested by our phylogenetic analysis that *Phileosimias* and *Bugtipithecus* are more closely related to Afro-Arabian anthropoids than to Asian anthropoids (supplementary materials). Ma, million years ago.

favored strepsirhines over haplorhines. Ecologically, strepsirhines were the only Asian primates to occupy those niches available to primates of relatively large body mass because medium and large haplorhine taxa such as amphipithecids were eradicated across the EOT in Asia. This pattern of turnover across the EOT among Asian primates differs radically from that which has been observed in Afro-Arabia. There, only small strepsirhines survived the EOT, whereas anthropoid haplorhines diversified to occupy a range of body sizes that was nearly an order of magnitude larger than their previous distribution (Fig. 4). The divergent responses shown by Afro-Arabian and Asian primates across the EOT set the stage for subsequent macroevolutionary patterns within this group. Africa became the geographic nexus of anthropoid evolution, whereas Asia continued to harbor sivaladapid strepsirhines and tarsiid haplorhines. Dynamic changes to the Asian physical environment during the interval spanning the EOT included progressive retreat of the Paratethys Sea from central Asia, continued uplift of the Tibetan-Himalayan orogen, and opening of the South China Sea (*24*). Africa was not immune to global climatic changes across the EOT, but it did not experience the dramatic tectonic and paleogeographic alterations that characterized Asia at this time. It is tempting to attribute the different patterns of turnover in Asian and African primate faunas across the EOT to local changes in vegetation and paleoenvironment (*25*), but current evidence is not sufficient to rule out the possibility that stochastic processes also played a substantial role.

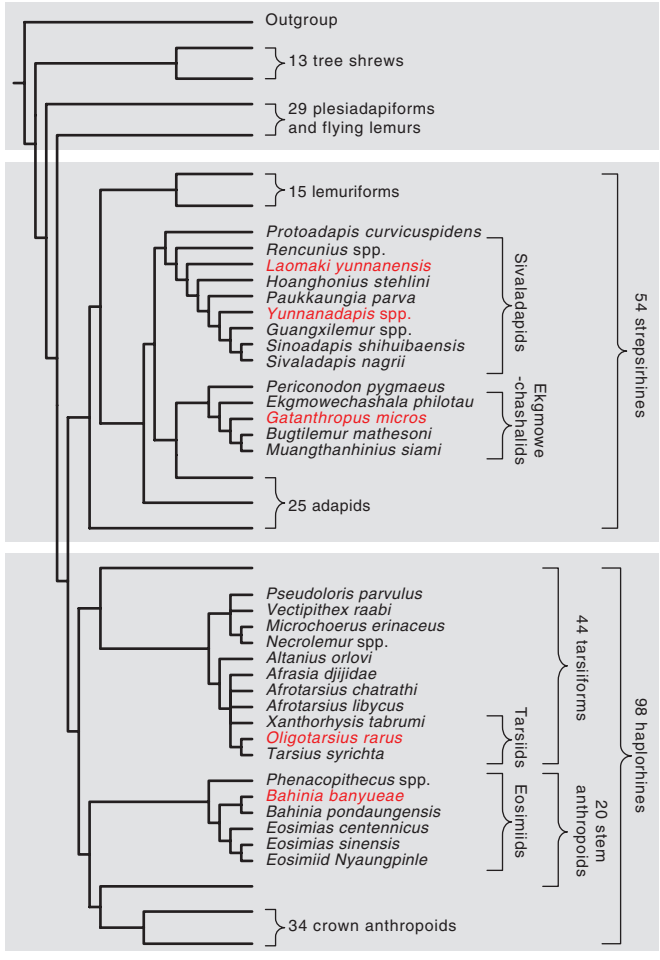

Fig. 3. Summary phylogeny of 196 mammals. Parsimony analysis is based on a data matrix that includes 1227 morphological characters and 663 molecular characters of long and short interspersed nuclear elements scored for 149 fossil and 47 living taxa. The topology of extant treeshrews, flying lemurs, and primates used as a backbone constraint or "molecular scaffold" is based on a gene supermatrix (supplementary materials).

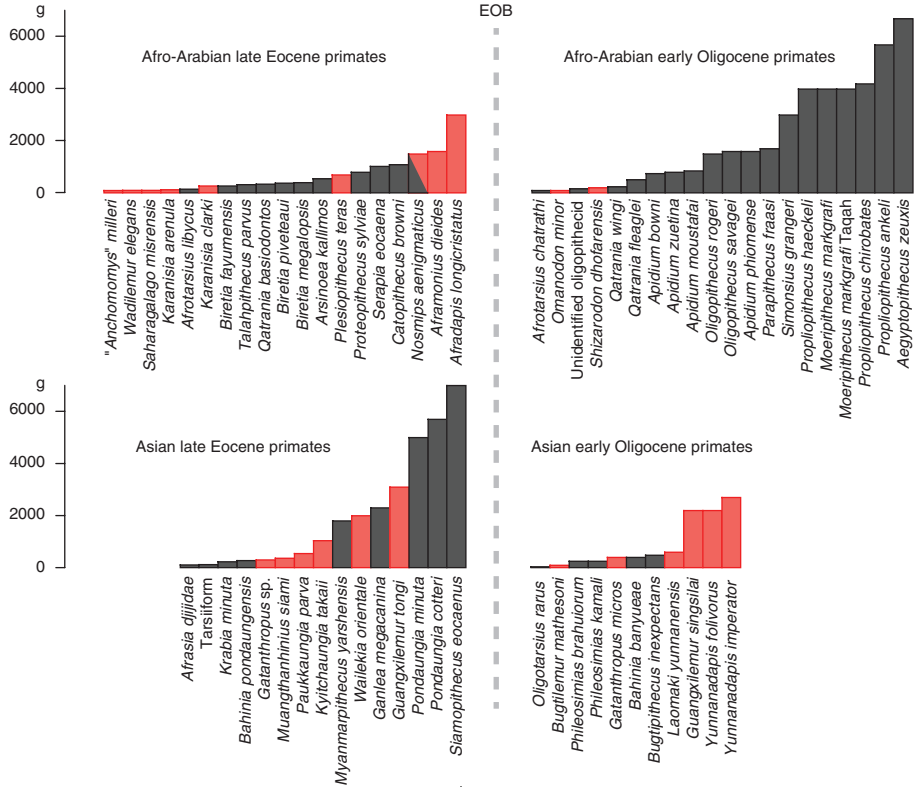

Fig. 4. Body-mass spectrum of fossil primates across the EOB in Afro-Arabia and southern Asia. Gray bars represent haplorhines. Pale red bars represent strepsirhines. *Nosmips* is uncertain (*26*). Later Eocene Afro-Arabian anthropoids occupy the middle of the spectrum. Later Eocene Afro-Arabian strepsirhines dominate the two extremes. Early Oligocene Afro-Arabian strepsirhines are restricted to the small end of the body-size distribution. Early Oligocene Afro-Arabian anthropoids span most of the body-mass range. Later Eocene Asian strepsirhines occupy the middle part of the body-mass spectrum. Later Eocene Asian anthropoids dominate the small and large body-mass areas. Early Oligocene Asian anthropoids are restricted to the small body-mass area. Early Oligocene Asian strepsirhines continue to occupy a broad range of body masses. Data are listed in table S2.

REFERENCES AND NOTES

1. X. Ni, Y. Hu, Y. Wang, C. Li, *Anthropol. Sci.* **113**, 3–9 (2005).
2. K. C. Beard, *Proc. Natl. Acad. Sci. U.S.A.* **105**, 3815–3818 (2008).
3. M. Köhler, S. Moyà-Solà, *Proc. Natl. Acad. Sci. U.S.A.* **96**, 14664–14667 (1999).
4. E. R. Seiffert, *Folia Primatol. (Basel)* **78**, 314–327 (2007).
5. I. S. Zalmout *et al.*, *Nature* **466**, 360–364 (2010).
6. E. R. Seiffert, *Evol. Anthropol.* **21**, 239–253 (2012).
7. N. J. Stevens *et al.*, *Nature* **497**, 611–614 (2013).
8. J. Meng, M. C. McKenna, *Nature* **394**, 364–367 (1998).
9. J. Sun *et al.*, *Sci. Rep.* **4**, 7463 (2014).
10. X. Ni, K. C. Beard, J. Meng, Y. Wang, D. L. Gebo, *Am. Mus. Novit.* **3571**, 1–11 (2007).
11. B. Wang, *Vertebrata PalAsiatica* **46**, 81–89 (2008).
12. X. Ni *et al.*, *Proc. R. Soc. B Biol. Sci.* **277**, 247–256 (2010).
13. K. C. Beard, T. Qi, M. R. Dawson, B. Wang, C. Li, *Nature* **368**, 604–609 (1994).
14. K. C. Beard *et al.*, *Proc. R. Soc. B Biol. Sci.* **276**, 3285–3294 (2009).
15. L. Marivaux *et al.*, *Science* **294**, 587–591 (2001).
16. L. Marivaux, J. L. Welcomme, S. Ducrocq, J. J. Jaeger, *J. Hum. Evol.* **42**, 379–388 (2002).
17. L. Marivaux *et al.*, *Proc. Natl. Acad. Sci. U.S.A.* **102**, 8436–8441 (2005).
18. O. Maridet, X. Ni, *J. Vertebr. Paleontol.* **33**, 185–194 (2013).
19. J. Jaeger *et al.*, *Science* **286**, 528–530 (1999).
20. K. C. Beard, J. Wang, *J. Hum. Evol.* **46**, 401–432 (2004).
21. P. D. Gingerich, A. Sahni, *Nature* **279**, 415–416 (1979).
22. X. Ni, in *Palaeovertebrata Sinica. Volume III. Basal Synapsids and Mammals. Fascicle 3 (Serial no. 16). Eulipotyphlans, Proteutheres, Chiropterans, Euarchontans, and Anagalids*, C. Li, Z. Qiu, Eds. (Science Press, 2015), pp. 284–389.
23. J. X. Samuels, L. B. Albright, T. J. Fremd, *Am. J. Phys. Anthropol.* **158**, 43–54 (2015).
24. A. Licht *et al.*, *Nature* **513**, 501–506 (2014).
25. R. J. Morley, in *Tropical Rainforest Responses to Climatic Change*, M. Bush, J. Flenley, W. Gosling, Eds. (Springer-Verlag, ed. 2, 2011), chap. 1, pp. 1–34.
26. E. R. Seiffert *et al.*, *Proc. Natl. Acad. Sci. U.S.A.* **107**, 9712–9717 (2010).
27. Y. Chaimanee *et al.*, *Proc. Natl. Acad. Sci. U.S.A.* **109**, 10293–10297 (2012).

ACKNOWLEDGMENTS

This project has been supported by the Strategic Priority Research Program of CAS (CAS, XDB03020501), the National Basic Research Program of China (2012CB821904), the CAS 100-talent Program, the National Natural Science Foundation of China (41472025), and the U.S. National Science Foundation (BCS 0820602, BCS 1441585, and EAR 1543684). We thank Z. Yan, G. Wang, R. Li, and G. Li for their assistance in the field. The phylogenetic data used in the paper are archived in the supplementary materials.

SUPPLEMENTARY MATERIALS

www.sciencemag.org/content/352/6286/673/suppl/DC1
Materials and Methods
Systematic Paleontology
Measurements
Body Mass Estimation
Phylogenetic Analysis
Figs. S1 to S10
Tables S1 and S2
References (*28*–*63*)
Databases S1 and S2

7 January 2016; accepted 24 March 2016
10.1126/science.aaf2107

ASTROPARTICLE PHYSICS

Observation of the ^{60}Fe nucleosynthesis-clock isotope in galactic cosmic rays

W. R. Binns,[1]* M. H. Israel,[1]* E. R. Christian,[2] A. C. Cummings,[3] G. A. de Nolfo,[2] K. A. Lave,[1] R. A. Leske,[3] R. A. Mewaldt,[3] E. C. Stone,[3] T. T. von Rosenvinge,[2] M. E. Wiedenbeck[4]

Iron-60 (^{60}Fe) is a radioactive isotope in cosmic rays that serves as a clock to infer an upper limit on the time between nucleosynthesis and acceleration. We have used the ACE-CRIS instrument to collect 3.55×10^5 iron nuclei, with energies ~195 to ~500 mega–electron volts per nucleon, of which we identify 15 ^{60}Fe nuclei. The ^{60}Fe/^{56}Fe source ratio is $(7.5 \pm 2.9) \times 10^{-5}$. The detection of supernova-produced ^{60}Fe in cosmic rays implies that the time required for acceleration and transport to Earth does not greatly exceed the ^{60}Fe half-life of 2.6 million years and that the ^{60}Fe source distance does not greatly exceed the distance cosmic rays can diffuse over this time, ≲1 kiloparsec. A natural place for ^{60}Fe origin is in nearby clusters of massive stars.

Signature of recent nucleosynthesis

The radioactive isotope ^{60}Fe [which decays by β^- decay with a half-life of 2.62×10^6 years (*1*)] is expected to be synthesized and ejected into space by supernovae, and thus could be present in galactic cosmic rays (GCRs) near Earth, depending upon the time elapsed since nucleosynthesis and the distance of the supernovae. ^{60}Fe is believed to be produced primarily in core-collapse supernovae of massive stars with mass $M >$ ~10 solar masses ($M_\odot$), which occur mostly in associations of massive stars (OB associations). It is the only primary radioactive isotope with atomic number $Z \leq 30$ [with the exception of ^{59}Ni, for which only an upper limit is available (*2*)] produced with a half-life long enough to potentially survive the time interval between nucleosynthesis and detection at Earth. (Primary cosmic rays are those that are synthesized at the GCR source, as opposed to secondary cosmic rays, which are produced by nuclear interactions in the interstellar medium.) ^{60}Fe is difficult to measure with present-day instruments because of its expected extreme rarity, based on nucleosynthesis calculations for supernovae (*3*, *4*). The detection of ^{60}Fe in cosmic rays would be a clear sign of recent, nearby nucleosynthesis. The long period of data collection (17 years) achieved by the Cosmic Ray Isotope Spectrometer (CRIS) aboard NASA's Advanced Composition Explorer (ACE) (*5*), the excellent mass and charge resolution of the CRIS instrument, and its capability for background rejection have enabled us to detect ^{60}Fe.

^{60}Fe has been detected in other samples of matter. Measurements of diffuse γ-rays from the interstellar medium (ISM) by the spectrometer on the International Gamma-Ray Astrophysics Laboratory (INTEGRAL) spacecraft have revealed line emission at 1173 and 1333 keV from ^{60}Co, the daughter product of ^{60}Fe decay, clear evidence that "nucleosynthesis is ongoing in the galaxy" (*6*). As expected, this emission is diffuse instead of point-like, since the ^{60}Fe lifetime is sufficiently long to allow it to diffuse over distances that are large compared to the size of a supernova remnant. This is one of many strong connections between γ-ray astronomy and direct cosmic-ray studies (*7*).

Deep-sea manganese crusts from two different locations have also been found to harbor elevated ^{60}Fe levels (*8*, *9*). Analysis of crust layers using accelerator mass spectrometry showed significant increases in the ^{60}Fe/Fe ratio 2.8 million years (My) ago, "compatible with deposition of supernova ejecta at a distance of a few tens of pc" (*9*). The measurement was verified by an independent analysis (*10*), although these investigators did not find a corresponding increase in a marine-sediment sample [see (*10*, *11*) for discussion]. We note that the manganese crust studies (*8*–*10*) used outdated half-lives for ^{60}Fe and ^{10}Be—1.49 and 1.51 My , respectively—instead of the currently accepted 2.62 and 1.387 My (*1*). Using these recent lifetimes, it has been estimated that the peak in the ^{60}Fe/Fe ratio (*9*) as a function of depth corresponds to an age of 2.2 My (*11*). Lunar surface samples also show elevated ^{60}Fe/Fe ratios consistent with supernova debris arriving on the Moon ~2 My ago (*12*, *13*). These deep-sea manganese crust and lunar surface observations were compared with expectations from possible stellar sources (*11*) and found to be consistent with an origin in core-collapse supernovae, but inconsistent with Type Ia supernovae, which produce orders of magnitude less ^{60}Fe.

Cosmic-ray ^{60}Fe detection

The CRIS instrument was launched on ACE in 1997 and has operated continuously since that

[1]Washington University, St. Louis, MO 63130, USA. [2]NASA/Goddard Space Flight Center, Greenbelt, MD 20771, USA. [3]California Institute of Technology, Pasadena, CA 91125, USA. [4]Jet Propulsion Laboratory, California Institute of Technology, Pasadena, CA 91109, USA.
*Corresponding author: Email: wrb@wustl.edu (W.R.B.); mhi@wustl.edu (M.H.I.)

Oligocene primates from China reveal divergence between African and Asian primate evolution

Xijun Ni, Qiang Li, Lüzhou Li and K. Christopher Beard

Science **352** (6286), 673-677.
DOI: 10.1126/science.aaf2107

Climate filters dominant species

The transition between the Eocene and Oligocene periods was marked by distinct cooling. Because primate species are particularly susceptible to cold, this change in climate drove a retraction of primates globally. After this transition, anthropoid primates were dominant in Afro-Arabian regions, but little has been known about primate reestablishment in Asia. Ni *et al.* describe 10 previously unknown primates found in Yunnan Province in China that show that primates took a different path in Asia. Instead of anthropoids, strepsirrhine (lemur-like) primates were dominant. It is still unknown whether this difference was due to the environment or chance.

Science, this issue p. 673